The 2010 IEEE/RSJ International Conference on
Intelligent Robots and Systems
October 18-22, 2010, Taipei, Taiwan

Calibration of a rotating multi-beam Lidar

Naveed Muhammad[1,2] and Simon Lacroix[1,2]

Abstract— **This paper presents a technique for the calibration of multi-beam laser scanners. The technique is based on an optimization process, which gives precise estimation of calibration parameters starting from an initial estimate. The optimization process is based on the comparison of scan data with the ground truth environment. Detailed account of the optimization process and suitability analysis of optimization objective function is described, and results are provided to show the efficacy of calibration technique.**

I. INTRODUCTION

Multi-laser scanning systems are very interesting for applications in autonomous mobile robotic systems, because they can provide 3D information about their environments in real-time therefore and can efficiently be used for tasks such as environment modeling, obstacle detection, and SLAM. One of these systems is the Velodyne HDL-64E S2: it consists of 64 lasers located on a spinning head which can spin at a rate of 5 to 15 Hz, and provides 3D data about its surroundings at a rate of 1.33 million points per second. Another such system is Ibeo LUX which scans its surroundings in four parallel layers.

The performance of these scanners strongly depends on their calibration. Indeed, precise 3D data from an environment can easily be processed to extract linear or planar features, whereas extraction of these features can be difficult, unreliable or impossible if the sensor is badly calibrated. Similarly, imprecise calibration can result in inaccurate digital terrain maps, and thus erroneous interpretations of the sensed terrain.

This paper provides a technique for the calibration of a rotating multi-beam lidar. An optimization technique is employed to estimate the calibration parameters more precisely. Starting from a coarse initial calibration, data acquired by the scanner is compared to the ground truth environment to precisely estimate calibration parameters. The paper is organized as follows: section II discusses related work, section III defines the various “ingredients” required by a lidar calibration process, and section IV presents the implementation of the proposed calibration technique on a real multi-beam lidar system and also presents some results.

II. RELATED WORK

A lot of work has been done on the calibration of cameras, multi-camera systems and omni-directional vision sensors. *E.g.* [1] is a widely used tool for the calibration of intrinsic and extrinsic calibration of cameras. Calibration techniques for multi-laser sensors, however, have not been investigated to that extent. [2] provide a technique for extrinsic calibration (*i.e.* estimation of the rotation and translation parameters between the sensor frame and the robot body frame) of a Sick lidar mounted on a mobile robot. Starting from a set of inaccurate hand-measured extrinsic calibration parameters, they present an optimization based calibration technique which adjusts the calibration parameters by comparing scan data and a ground-truth environment. Extensions of the technique to incorporate multiple Sick laser scanners, and a set of heterogeneous sensors are presented in [3] and [4].

In [5] a procedure for calibrating only the additive and proportional distance correction factors of a multi-beam laser scanner is described. [6] mention the calibration of distance correction parameters for a multi-laser scanner by comparing its distance readings to those from a Sick lidar but do not provide any details on the calibration procedure. In range imaging using time-of-flight cameras, similar “distance correction” calibration parameters exist. [7] calibrate these parameters by making a look-up table for the operational range of device. [8] calibrate these parameters by fitting a B-spline to the measurement errors made by camera at different distances in the operational range.

So far a generic technique for intrinsic calibration of multi-beam lidars has not been proposed to our knowledge. In this paper, we present such a technique which is based on an optimization process similar to the extrinsic calibration technique proposed in [4]. The lidar model we use is somewhat similar to general imaging models, in which the camera is not modelled as pin-hole central projection, but as a set of 3D lines without any single viewpoint constraint [9]. The calibration process then becomes to estimate the parameters of the supporting line associated to each laser beam.

III. APPROACH

A multi-beam lidar system is modelled as a set of rays, *i.e.* straight lines. These rays define the position and orientation of laser beams in a sensor-fixed coordinate frame. The intrinsic calibration for such systems is the estimation of parameters that define the position and orientation of each of the laser beams. The principle underlying the calibration technique proposed in this paper is an optimization process performed to estimate the lidar calibration parameters so that the 3D data acquired by lidar matches the ground truth.

Starting from a coarse measurement of calibration parameters for laser beams, we can convert the raw scan data into a 3D point cloud. A calibration environment can be designed and constructed to acquire lidar data for calibration. The selection of a suitable calibration environment depends on the system at hand and parameters to be calibrated,

1: CNRS ; LAAS ; 7 avenue du colonel Roche, F-31077 Toulouse, France
2: Université de Toulouse ; UPS , INSA , INP, ISAE ; LAAS ; F-31077 Toulouse, France
firstname.lastname@laas.fr

978-1-4244-6676-4/10/$25.00 ©2010 IEEE

and also on practicalities like simplicity in its structure and construction. For example a simple planar surface might be suitable for calibration of the orientation of a laser beam but will not suffice for the estimation of its position. The scenario changes if the edges of the scanned planar surface are also taken into account: by introducing the fact that the edges must correspond to straight lines, we can also optimize the position parameters of a laser beam.

Another possibility can be using a straight pole. Performing optimization on the scans of such a structure intuitively seems appropriate to estimate position and orientation parameters of a laser beam, but in practice issues like the small width of the pole result in insufficient data to perform optimization – and larger poles would require fitting a cylinder to the scan data and not a straight line. Another cause for insufficient data in this case is the decrease in resolution of scan-data as the distance of scanned object increases. Another very important factor to be taken into account during calibration process is that calibration estimates should not be biased on distances. This creates the need of scan data used for performing calibration to cover objects at varying distances from the sensor.

The rest of the section depicts the required steps to set up a calibration process.

A. *Choice of parameterization*

A very basic requirement for the calibration process is the choice of the parameters that define the position and orientation of a laser beam in the multi-beam lidar system. This choice depends on the physical setting of system at hand, but also on practical issues, like a priori availability of coarse calibration data for the system: if one has a coarse calibration for the device, one might decide to stick to the parameterization used in this coarse calibration and improve it. Lets define this set of parameters by $\{M_1, \ldots, M_n\}$.

At least five parameters are required to define one laser beam in a 3D coordinate frame: two angles to define the direction of the associated line and three parameters to define the point origin of the beam. If an additive and/or proportional distance correction factor is required to correct the measurement made by laser beam, the number of calibration parameters goes to six or seven per laser beam.

In practice however the exact location of the laser beam origin is not required and therefore the additive distance correction factor can be incorporated into the three parameters defining the position of laser beam. For example, to incorporate an additive distance correction factor of 1m, the point of origin of laser beam can be considered shifted 1m along the laser beam.

Another possibility to parametrize a laser beam is by using two angles and two distance parameters defining an infinitely long line. A fifth parameter, an additive distance correction factor completes the knowledge for converting a raw lidar measurement to a 3D point. This parametrization is used for the calibration implementation in this paper and is depicted in section IV-A.

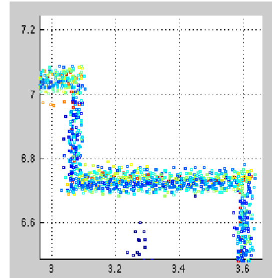

Fig. 1. Top view of a corner in a room (units in m)

B. *Choice of objective function*

The chosen calibration environment must also allow the selection/definition of an objective/cost function C. This function forms the basis of the optimization process and is used to quantitatively compare the acquired 3D point cloud data and the real environment. C should provide higher costs if there is more difference between the acquired 3D data and ground-truth environment, and lower costs as the match between acquired 3D data and real environment improves. Another important requirement for C is that it should be sensitive to each of the parameters to be optimized. It means that the cost provided by this function must vary with the values of the parameters to be optimized, and of course this increase or decrease in the cost should be in accordance with the first criteria for C *i.e.* the cost should be lower for better matches between the acquired 3D data and ground truth and vice versa. The suitability of the cost function to perform a successful calibration process can be analyzed by computing the partial derivatives of the cost function with respect to the parameters to be optimized. In order for the cost function to be suitable, these partial derivatives should generally be non-zero and non-constant (more explanation in subsection IV-C.3).

$$\partial C / \partial M_i \neq constant \tag{1}$$

C. *Choice of minimization technique*

A basic choice during a calibration process is the formulation of optimization as a constrained or unconstrained minimization problem. The choice depends on the range in which the calibration parameters are expected to lie. The process can be formulated as a constrained problem if the calibration parameters are sure to lie in a specific range. Moreover a suitable minimization algorithm can be chosen from a range of available mathematical algorithms.

D. *Data segmentation*

Data segmentation consists in extracting, from acquired data, the data that actually correspond to the calibration object for which the ground truth is known. Fig. 1 shows the top view of a region in a room. For the three corner regions in the figure, it is very hard to segment the data, *i.e.* to associate the data point to one or the other wall. The environment chosen for the calibration process should be designed and made to allow appropriate segmentation of data.

IV. IMPLEMENTATION

This section presents the implementation of the calibration technique on a multi-beam lidar system. The device is a Velodyne HDL-64E S2 [10]. It has 64 lasers embedded in a spinning head. The lasers are grouped in two blocks, with 32 located in the upper block and the remaining 32 in the lower block of the lidar spinning head. Lasers in each block are further divided into two groups of 16 lasers each, one group located rightwards and the other leftwards.

A. Geometric model

Each of the 64 lasers in the device is characterized by five parameters that are required to convert the distance value returned by the laser to 3D point coordinates. These parameters are (Fig. 2 and Fig. 3):

- Distance Correction Factor D_{corr}: value to be added in the distance returned by corresponding laser D_{ret} to get the real distance value D.
- Vertical Offset V_o: distance measured orthogonal to the laser beam, representing the distance of laser beam from origin in a vertical sense – segment OA in Fig. 3 (top) where O is the origin of sensor-fixed frame.
- Horizontal Offset H_o: horizontal counterpart of V_o – segment OB in Fig. 3 (bottom).
- Vertical Correction Angle θ: angle made by the laser beam with x-y plane, as shown in Fig. 3 (top). *E.g.* for a laser beam lying in y-z plane, this would be the angle made by laser beam around x-axis.
- Rotational Correction Angle α: angle made by the laser beam with y-z plane (not shown on the figure).

As the lidar head spins, its current rotational angle is denoted as ϕ. Each laser has a different value of α so we can define another angle β such that $\beta = \phi$ - α. In this way β represents the orientation of laser beam relative to the current rotational angle of spinning lidar head.

The distance values returned by a single laser (D_{ret}) can be converted to a 3D point P with Cartesian coordinates $(P_x, P_y, P_z)^T$ expressed in lidar frame, using the above five parameters and the current rotational angle of lidar head:

$$D = D_{ret} + D_{corr} \tag{2}$$

$$D_{xy} = D * \cos(\theta) - V_o * \sin(\theta) \tag{3}$$

$$P_x = D_{xy} * \sin(\beta) - H_o * \cos(\beta) \tag{4}$$

$$P_y = D_{xy} * \cos(\beta) + H_o * \sin(\beta) \tag{5}$$

$$P_z = D * \sin(\theta) + V_o * \cos(\theta) \tag{6}$$

Among the five calibration parameters D_{corr}, α and θ are the most important. This is because of the fact that errors induced by a bad estimate of these parameters in the precision of 3D coordinates of acquired data changes with the distance of scanned object/surface, whereas the errors induced by imprecise calibration of V_o and H_o do not depend on the variation in the distance of scanned object. Therefore in this paper we concentrate on the calibration of D_{corr}, α and θ – but the same principle can be applied to the calibration of other two parameters.

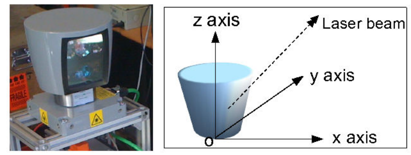

Fig. 2. Velodyne HDL-64E S2 (left) and sensor-fixed frame (right)

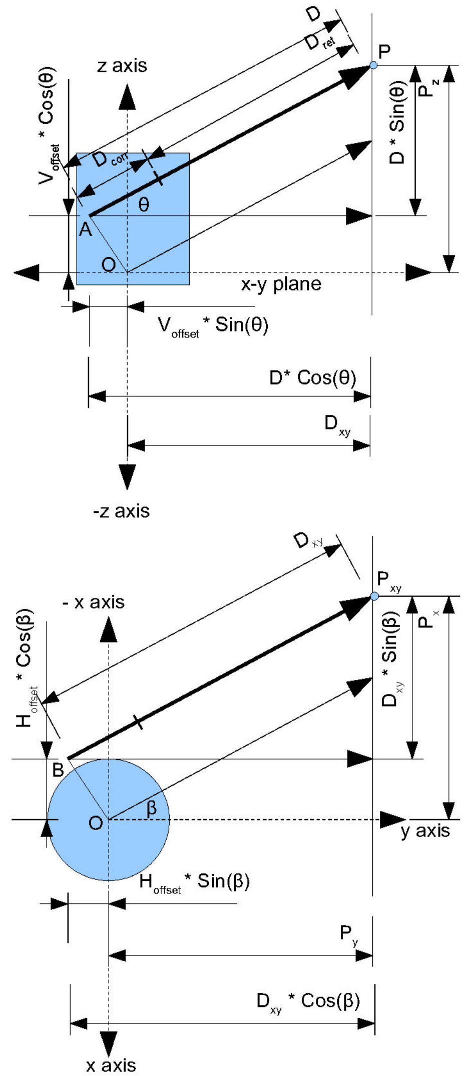

Fig. 3. Lidar unit's side-view (top) and top-view (bottom)

B. Sensor characterization

The device comes with a set of calibration parameters. In practice these default calibration parameters are not very accurate. Fig. 4 shows one example of this inaccurate calibration. The figure shows segmented view of a planar surface placed at 3m distance from the lidar. Each horizontal line in the scan shows the data from a single laser. One can see that the data from all the lasers are not aligned to form a rectangular planar surface, instead the data from different lasers are horizontally misaligned. This misalignment seems to be repeated between every two consecutive lasers which come from right and left sided blocks on the lidar head. Fig.

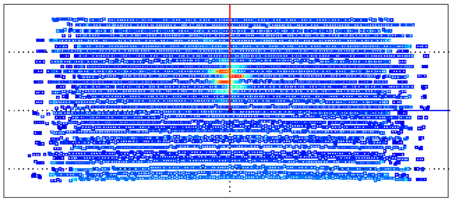

Fig. 4. A planar surface, seen from front

TABLE I

NOISE DIFFERENCE BETWEEN TWO LASERS BEAMS

Mean	Standard Deviation	Maximum Difference
13.68m	0.74cm	3cm
13.68m	0.53cm	2cm

1 shows another effect of inaccurate calibration: ideally, if the calibration parameters for all lasers were accurate and the sensor had lower noise, as seen from top the walls should have looked much thinner and corners much sharper.

Another factor affecting the accuracy of scan data is the internal (electronic) noise of the sensor. This internal noise also defines the lower bound on noise level with a very precise calibration. Fig. 5 (top) shows a histogram for 37 consecutive scans of the same point from a single laser with almost 0° view angle. We can see that the depth measurement changes slightly between the readings. The figure also shows the mean (red) and 2 x standard deviation bounds (green). The standard deviation in this case is about 0.75 cm and the maximum difference between any two measurements is 2.6 cm. We can see that the measurements always lie within 2 x standard deviation bound. Fig. 5 (bottom) shows a similar histogram for a point scanned with a view angle of 6°. Here the standard deviation was recorded to be 1.4 cm and the maximum difference between any two readings was 6.2 cm. Moreover some data points lie outside the 2 x standard deviation bound. One reason for this decrease in the accuracy of scan data is the increase in view angle.

The internal noise also varies from laser to laser within the device. Table I shows the difference between the data from two lasers viewing a point, with approximately same scan distance and angle.

C. Calibration process

1) Calibration Environment: Keeping in view the environment selection issues discussed in section III, a 4.40m wide planar wall is used as the calibration environment. The wall is scanned by placing the lidar at multiple distances: distances range from 4 to 14m with 2m steps. This has been done twice, once by approximately aligning the wall to the $x-axis$ of lidar's fixed frame and then by aligning it to lidar's $y-axis$. Therefore a total of 12 scans of the wall were used in the calibration process. The alignment of the wall to the lidar x and y axes is not necessary and was just approximate. The distribution of scan data over a range of distances is very important. Sufficiently distributed data is necessary to ensure the estimation of calibration parameters

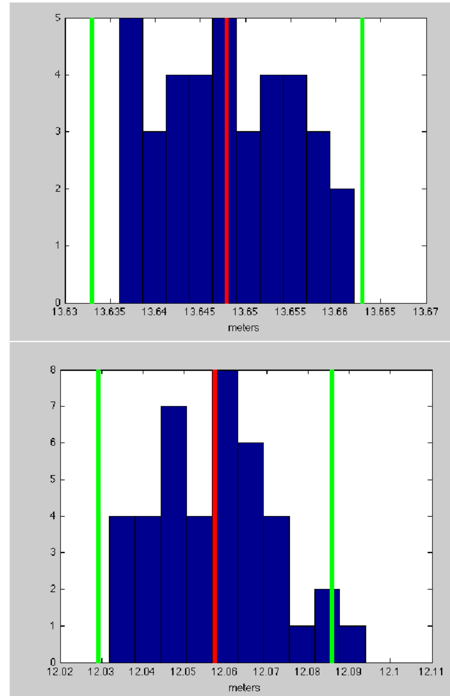

Fig. 5. Histogram for 37 consecutive scans of a point with 0° (top) and 6° (bottom) view angles, mean(red) and 2 x standard deviation(green)

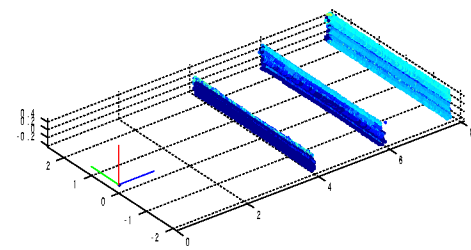

Fig. 6. Three scans with wall aligned to y-axis of lidar's fixed frame

to be independent of any bias on a specific distance. Fig. 6 shows three of the 12 scans of the wall superimposed in a single plot.

2) Cost function: If it is possible to accurately align the planar surface to be scanned, the cost function C can be defined as the variance of 3D data along the plane normal: when the wall is scanned with the lidar's y axis aligned to the wall, the cost is the average squared difference between the mean distance x_{mean} and each distance x:

$$C_y = \Sigma(P_{x,i} - P_{x,mean})^2/n \quad (7)$$

where C_y represents the cost of a scan when the wall was aligned to $y-axis$ of lidar's fixed frame, and n is the total number of points in the current scan. Similarly C_x i.e. cost of a given scan when the wall was aligned to $x-axis$ of lidar's fixed frame is given by:

$$C_x = \Sigma(P_{y,i} - P_{y,mean})^2/n \quad (8)$$

In practice it is hard to accurately align the plane with the x or y of the lidar frame. Therefore during our optimization process, at each iteration a PCA based plane fitting is performed to estimate the parameters of the plane that best define the 3D points in the scan. The cost function C is therefore chosen to be the sum of squared perpendicular-distances of all points in the plane divided by the total number of points forming the plane.

$$C = \Sigma (D_{i,Perp})^2 / n \tag{9}$$

where n is the total number of points in current scan of the plane (wall).

Section IV-D compare the results obtained with and without this plane fitting process.

3) Suitability analysis and optimization: As mentioned in section III, the suitability of the cost function for optimization depends on the cost function sensitivity to the variation of the parameters to be estimated. As our chosen cost function depends on the distances of x, y and z coordinates of 3D data, the suitability of chosen cost function can be ensured by finding the partial derivatives of P_x, P_y and P_z with respect to each of the three calibration parameters to be optimized, *i.e.* D_{corr}, α and θ.

Using equations 4, 5 and 6, the partial derivatives with respect to D_{corr} are given as:

$$\partial P_x / \partial D_{corr} = \cos\theta \sin\beta \tag{10}$$

$$\partial P_y / \partial D_{corr} = \cos\theta \cos\beta \tag{11}$$

$$\partial P_z / \partial D_{corr} = \sin\theta \tag{12}$$

From $\partial P_x / \partial D_{corr}$ it is clear that the conditions that make the partial derivative equal to zero are $\theta = 90°$ and $\beta = 0°$. This makes intuitive sense as $\theta = 90°$ means that the laser is pointing upwards and in such a situation it is impossible to scan a plane (wall) which is parallel to the laser. Similarly, as β defines the current orientation of a laser beam, $\beta = 0°$ means that the laser is parallel to $y-axis$ of lidar frame and therefore any variation in D_{corr} would not affect P_x for the point being viewed as β remains 0°. In our case as the lidar is constantly rotating, the value of β is constantly changing, and moreover the values for θ for all lasers in the lidar are much smaller than 90°.

Similarly, the conditions that make $\partial P_y / \partial D_{corr}$ equal to zero are $\theta = 90°$ and $\beta = 90°$. As with the previous case, the condition $\beta = 90°$ is not a problem because the lidar is constantly rotating as we acquire the data. The condition that makes $\partial P_z / \partial D_{corr}$ equal to zero is $\theta = 0°$. This would mean that for lasers with zero pitch angle, the z coordinates of data points will not play any role in the optimization process. This does not pose any problem because the optimization process is based on 3D data and not only on the z coordinates of data. Moreover for the system at hand, the pitch angle for any laser beam is not exactly zero. This analysis leads us to the conclusion that our chosen cost function is suitable to be used for the estimation of D_{corr} using optimization.

The partial derivatives with respect to θ are given by:

$$\partial P_x / \partial \theta = -D \sin\beta \sin\theta - V_o \sin\beta \cos\theta \tag{13}$$

TABLE II

STANDARD DEVIATIONS (IN METERS) IN DEPTH OF PLANAR DATA

	Default Calibration	Recalibration
4m	0.0234	0.0215
6m	0.0326	0.0291
8m	0.0170	0.0116
10m	0.0168	0.0105
12m	0.0186	0.0119
14m	0.0187	0.0128

$$\partial P_y / \partial \theta = -D \cos\beta \sin\theta - V_o \cos\beta \cos\theta \tag{14}$$

$$\partial P_z / \partial \theta = -D \cos\theta - V_o \sin\theta \tag{15}$$

The conditions which make $\partial P_x / \partial \theta$ and $\partial P_y / \partial \theta$ equal to zero are $\beta = 0°$ and $\beta = 90°$ respectively. As with the case for D_{corr}, for the constantly rotating lidar, these partial derivatives remain non-zero for the type of 3D datasets we are using. Therefore our chosen cost function is suitable to be used for the estimation of θ using optimization. Similarly it can be shown that our cost function is also suitable for the optimization of the third calibration parameter α.

The optimization process was implemented using Matlab function $fmincon$ [11]. The computational cost of optimization process is not of a great concern because the process is done offline and has to be done only once to calibrate the device. Our optimization process took a few hours to complete on a normal laptop machine.

D. Results

The optimization was performed starting from the default calibration data provided by the manufacturer. One way to quantitatively assess the improvement in the optimized calibration parameters is to compare the standard deviations in the depth of planar data for default and optimized calibration parameters. Table II shows the improvements of these standard deviations in depth for a subset of planar data used for optimization.

Fig. 7 presents an example of improved scan results using re-estimated calibration parameters. At top, the figure shows the scan of the rear of a vehicle computed using default calibration data and at bottom it shows the same scan using optimized calibration parameters.

It is important to validate the optimized calibration parameters for data which is not used in the optimization process. Table III shows the improvement in standard deviations for depth of planar data when the wall is scanned from the distances of 16 and 18m, and these sets were not used in the optimization process. In the last column, the table shows the improvement in standard deviations in depths when the optimization is not done using plane fitting, but by trying to properly align the wall with x and y $axes$ of lidar frame as mentioned in section IV-C.2. We can see that the calibration has improved but not as much as in the case of using plane fitting. This is because of the fact that it is very hard to precisely align the scanned plane, and thus the alignment assumption is not valid in a strict sense.

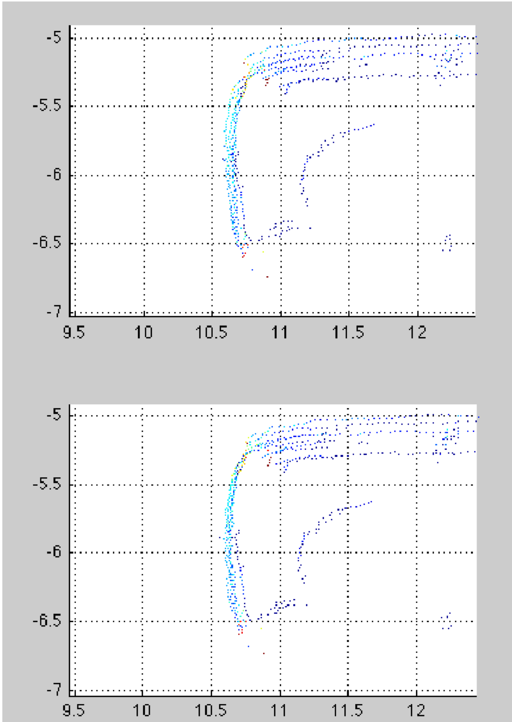

Fig. 7. Comparing default (top) and optimized (bottom) calibration parameters, scans of rear of a vehicle

TABLE III

STANDARD DEVIATIONS (IN METERS) FOR DATA NOT USED IN OPTIMIZATION

	Default Calibration	Recalibration	Recalibration (without plane fitting)
16m	0.0210	0.0132	0.0148
18m	0.0221	0.0142	0.0171

If the data used for optimization is not sufficiently distributed in terms of distance, the resulting estimation of calibration parameters can be highly biased on the distance at which the data used for optimization was taken. Table IV shows the change in standard deviations in depths of planar data when only the dataset taken by placing the lidar at 10m from the wall is used for the optimization process. For data at 10m, we have achieved a good improvement in the estimation of calibration parameters, But the important point here is that standard deviations for data at 4m actually become worse as a result of biased optimization process.

As pointed out in [5] and [6], often a proportional distance correction factor also exists for lidar devices similar to the one we used. For our device (Velodyne HDL-64E S2) however, neither the manufacturer mentioned the existence of such a factor nor was it found to exist during extensive experimentation with the device.

V. SUMMARY

Laser scanners are becoming more and more useful in the field of robotics. With recent innovations like the multi-beam lidars providing rich and fast 3D scans of the environment,

TABLE IV

BIASED ESTIMATION OF CALIBRATION PARAMETERS

	Default Calibration	Recalibration
4m	0.0312	0.0378
6m	0.0325	0.0301
8m	0.0200	0.0106
10m	0.0192	0.0064
12m	0.0190	0.0090
14m	0.0217	0.0117

these sensors have a great potential for being employed on mobile robots and changing the ways these robots sense and act in their environments. As for any other sensor, precise calibration is very important for these sensors to be useful. We have presented a technique for precise calibration of a rotating multi-beam lidar, and the principle can be extended to similar sensors. The paper has presented how optimization can be employed to perform precise calibration starting from a coarse set of calibration parameters. We now aim to work on the calibration of sensor frame with respect to the robot body frame, and possibly simultaneous calibration of multiple sensors *i.e.* lidars and cameras.

ACKNOWLEDGMENTS

This work has been partially funded by the Action project (action.onera.fr) and the ANR funded 2RT-3D project (www.pges.fr/2rt3d/).

REFERENCES

[1] J.-Y. Bouguet, *Camera Calibration Toolbox for Matlab*. [Online]. Available: http://www.vision.caltech.edu/bouguetj

[2] J. Underwood, A. Hill, and S. Scheding, "Calibration of range sensor pose on mobile platforms," in *IEEE/RSJInternational Conference on Intelligent Robots and Systems, SanDiego (CA), USA*, Oct. 2007.

[3] J. Underwood, "Reliable and safe autonomy for ground vehicles in unstructured environments," Ph.D. dissertation, The University of Sydney, Australia, December 2008.

[4] J. Underwood, A. Hill, T. Peynot, and S. Scheding, "Error modeling and calibration of exteroceptive sensors for accurate mapping applications," *Journal of Field Robotics*, vol. 27, no. 1, pp. 2–20, January/February 2010.

[5] P. Stone, P. Beeson, T. Mericli, and R. Madigan, "Darpa urban challenge technical report," Austin Robot Technology, Tech. Rep., 2007.

[6] J. Bohren, T. Foote, J. Keller, A. Kushleyev, D. Lee, A. Stewart, and P. Vernaza, "Little ben, the ben franklin racing team's entry in the 2007 darpa urban challenge," *Journal of Field Robotics*, vol. 25, pp. 598–614, 2008.

[7] T. Kahlmann and H. Ingensand, "Calibration for increased accuracy of the range imaging camera swissranger," in *IAPRS*, vol. XXXVI, September 2006, pp. 136–141.

[8] M. Lindner and A. Kolb, *Lateral and Depth Calibration of PMD-Distance Sensors*, ser. Lecture Notes in Computer Science. Springer Berlin/Heidelberg, 2006, vol. 4292/2006, pp. 524–533.

[9] P. Sturm and S. Ramalingam, "A generic concept for camera calibration," in *European Conference of Computer Vision*, vol. 2, 2004, pp. 1–13.

[10] *HDL 64E-S2 User's Manual – www.velodyne.com/lidar/*, Velodyne Lidar Inc, 345 Digital Drive, Morgan Hill, CA 95037, 2008.

[11] *Matlab Optimization Function: fnimcon*, The Mathworks Inc. [Online]. Available: http://www.mathworks.com/access/helpdesk/help/toolbox/optim/